ARTICLE

Intra- and Intermolecular Rovibrational States of HCl-H_2O and DCl-H_2O Dimers from Full-Dimensional and Fully Coupled Quantum Calculations[†]

Peter M. Felker[a*], Zlatko Bačić[b,c*]

a. Department of Chemistry and Biochemistry, University of California, Los Angeles, CA 90095-1569, USA
b. Department of Chemistry, New York University, New York 10003, USA
c. NYU-ECNU Center for Computational Chemistry at NYU Shanghai, Shanghai 200062, China

(Dated: Received on October 9, 2021; Accepted on October 31, 2021)

We report full-dimensional and fully coupled quantum bound-state calculations of the J=1 intra- and intermolecular rovibrational states of two isotopologues of the hydrogen chloride-water dimer, HCl-H_2O (HH) and DCl-H_2O (DH). The present study complements our recent theoretical investigations of the J=0 nine-dimensional (9D) vibrational level structure of these and two other H/D isotopologues of this noncovalently bound molecular complex, and employs the same accurate 9D permutation invariant polynomial-neural network potential energy surface. The calculations yield all intramolecular vibrational fundamentals of the HH and DH dimers and the low-energy intermolecular rovibrational states in these intramolecular vibrational manifolds. The results are compared with those of the 9D J=0 calculations of the same dimers. The energy differences between the K=1 and K=0 eigenstates exhibit pronounced variations with the intermolecular rovibrational states, for which a qualitative explanation is provided.

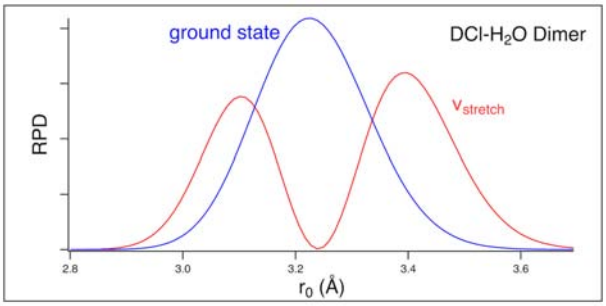

Key words: Weakly bound dimers, Rovibrational states, Quantum calculations

I. INTRODUCTION

Small hydrogen-bonded clusters of hydrogen chloride and water molecules have for decades been the subject of experimental and theoretical investigations [1]. This intense interest has been driven mainly by the opportunity that these clusters present for studying the fundamental aspects of important chemical processes in the atmosphere, ozone depletion being one of them. Moreover, clusters of hydrogen chloride with a variable number of water molecules afford a unique microscopic view of the first steps of hydration that ultimately result in the dissociation of HCl in bulk water [1, 2].

As the elementary constituent of the prototypical acid-water system, the hydrogen chloride–water dimer has particular importance. Consequently, it has been the focus of numerous high-resolution spectroscopic studies, that include microwave spectroscopy [3, 4], ragout-jet FTIR [5, 6] and infrared (IR) cavity ringdown spectroscopy [7] in the gas phase, and IR spectroscopy in liquid helium, as well as in nanodroplets [8–12]. The most investigated isotopologue has been the HCl-H_2O dimer. Its vibrational predissociation dynamics upon the excitation of the HCl stretch fundamental was studied experimentally [13, 14], leading to the determination of the dimer dissociation energy D_0=1334±10 cm^{-1} [13]. Some partially or fully deuterated isotopologues

[†]Part of Special Issue "John Z.H. Zhang Festschrift for celebrating his 60th birthday".

*Authors to whom correspondence should be addressed. E-mail: felker@chem.ucla.edu, zlatko.bacic@nyu.edu

 ©2021 Chinese Physical Society

of the hydrogen chloride–water dimer have been probed experimentally as well, by IR (DCl–D_2O) [6, 7] and microwave spectroscopies (DCl–H_2O, HCl–D_2O, DCl–D_2O [3], and analogous isotopologues involving HDO).

These experimental investigations have been complemented by a variety of theoretical treatments. From the electronic structure calculations over the years [15–19], it emerged that the HCl-H_2O dimer has the equilibrium structure with a near-linear hydrogen bond, in which HCl acts as the proton donor to the O atom of water as the proton acceptor. The geometry of this global minimum is non-planar, leading to two symmetrically equivalent pyramidal C_s structures (see FIG. 3 in Ref.[20]). A significant contribution to the theoretical description of the HCl-H_2O dimer was made by Mancini and Bowman [21], in the form of the *ab initio* based nine-dimensional (9D) potential energy surface (PES) of the dimer based on a permutationally invariant fit to over 44,000 CCSD(T)-F12b/aug-cc-pVTZ configurations and energies. This PES was used in the full-dimensional quantum diffusion Monte Carlo (DMC) calculations, which for the dimer's dissociation energy (D_0) gave the value of 1348±3 cm^{-1}, in good agreement with the experimental result [13]. What was still lacking at this point was a rigorous full-dimensional quantum calculations of the coupled excited inter- and intramolecular (ro)vibrational levels of the HCl-H_2O dimer.

This missing link was provided by our recently published theoretical study [20], which had two goals. One of them was introducing a new full-dimensional (9D) PES of the HCl-H_2O dimer, designated PES-2021, based on *circa* 43,000 data points computed at the level of CCSD(T)-F12a/aug-cc-pVTZ with the basis-set-superposition-error (BSSE) correction. The *ab initio* points were fit utilizing the ultraflexible permutation invariant polynomial-neural network (PIP-NN) approach [22–24]. The other goal was to present the first fully coupled 9D quantum calculations of the inter- and intramolecular vibrational states of the HCl-H_2O (HH) dimer, performed on PES-2021. These calculations characterized the vibrationally averaged non-planar ground-state geometry of the HCl-H_2O dimer, the intramolecular vibrational fundamentals of both monomers, and their frequency shifts relative to the gas-phase monomer values, together with the low-energy intermolecular vibrational states in each of the intramolecular vibrational manifolds and the manifestations of the coupling between the two sets of modes [20]. The properties calculated for the HCl-H_2O dimer turned out to be in excellent agreement with the spectroscopic data for the dimer in the literature. The dimer binding energy computed in 9D, D_0=1334.63 cm^{-1}, agrees extremely well with the experimental D_0 equal to 1334±10 cm^{-1} [13]. In addition, the ground-state expectation value of the out-of-plane bend angle of H_2O, 33.80°, and the HCl stretch frequency shift, −157.9 cm^{-1}, both from 9D calculations on PES-2021, are in very good accord with the corresponding experimental values for the dimer, 34.7° for the bend angle [4] and −161.9 cm^{-1} for the redshift of the HCl stretch fundamental [5, 7].

In the follow-up work [25], the rigorous full-dimensional investigation of the HH dimer in Ref.[20] was extended to three isotopologues of the hydrogen chloride-water dimer: DCl-H_2O (DH), HCl-D_2O (HD), and DCl-D_2O (DD). Its goal was to reveal the isotopologue variations of several bound-state properties of the hydrogen chloride-water dimer, and compare them to those of the HH dimer. These calculations also employed 9D PES-2021, and the same highly efficient fully coupled 9D quantum bound-state methodology. For the isotopologues in question, they yielded all intramolecular vibrational fundamentals, and their frequency shifted relative to the isolated monomer values, in combination with the low-lying intermolecular vibrational states in each of the intramolecular vibrational manifolds of interest. Moreover, for each isotopologue, important vibrationally averaged intermolecular geometric properties were computed for the dimer in the ground vibrational state, as well as the three rotational constants.

What enabled the extremely demanding 9D quantum bound-state calculations in the above studies is the methodology developed by us in Ref.[26]. It is the adaptation of the general approach for fully coupled quantum computation of intra- and intermolecular (ro)vibrational excitations of noncovalently bound molecular complexes [27] to weakly bound triatom-diatom dimers. The exceptional effectiveness of this methodology has two main sources. One of them is the surprising insight [27, 28] that fully coupled calculation of high-frequency intramolecular vibrational excitations in noncovalently bound systems can be accomplished by utilizing compact final basis sets with only a small number of low-lying intermolecular eigenstates whose energ-

DOI:10.1063/1674-0068/cjcp2110189 ©2021 Chinese Physical Society

ies are far below those of the intramolecular vibrational states of interest. This was rationalized by making a physically motivated assumption of extremely weak coupling between the intramolecular vibrational fundamentals and overtones and the very highly excited intermolecular states close in energy [27, 28]. Consequently, excluding the latter from the basis has no effect on the accuracy of the results. This results in a large reduction of the dimension of the basis set employed.

The other key factor is the computational strategy designed specifically to exploit the above insight. The full (ro)vibrational Hamiltonian of the dimer [20, 25–27, 29], 9D in the case of HCl-H_2O and the isotopologues, is partitioned into four terms: a (5D) rigid-monomer intermolecular vibrational Hamiltonian, two intramolecular vibrational Hamiltonians—one for the triatom (water) monomer (3D) and the other for the diatom (hydrogen chloride) moiety (1D), and a 9D remainder term. Each of the three reduced-dimension Hamiltonians is diagonalized separately and small portions of their low-energy eigenstates are included in a compact (9D) product contracted basis that covers all internal, intra- and intermolecular, degrees of freedom (DOFs) of the dimer. It is only because of the use of the contracted eigenstate basis for the intermolecular vibrational DOFs that fully coupled 9D quantum bound-state calculations of all intramolecular vibrational fundamentals of the noncovalently bound triatom-diatom complexes are possible. It enables straightforward selection of just a small number of lowest-energy intermolecular vibrational eigenstates for inclusion in the compact final 9D product contracted basis [27], in which the full (ro)vibrational Hamiltonian of the dimer is diagonalized.

The use of the eigenstates of reduced-dimension Hamiltonians to decrease the size of the final full-dimensional basis is not entirely new. Bačić and Light introduced the sequential diagonalization-truncation scheme [30–33], that proved very successful in the applications to fluxional molecules and molecular complexes such as LiCN/LiNC, HCN/HNC, $(HF)_2$ [34], $(HCl)_2$ [35], and others. For polyatomic molecules such as acetylene, H_2O_2, CH_4, and CH_5^+, Carter and Handy [36] and Carrington and co-workers [37, 38], implemented similar ideas of dividing the internal coordinates into two groups and using the eigenvectors of the corresponding reduced-dimension Hamiltonians in the final product contracted basis. In addition, monomer vibrational eigenstates of noncovalently bound complexes have been used as the contracted basis for the intramolecular vibrational DOFs of the complexes [39]. But, the basis for the intermolecular DOFs was not contracted in these studies. This omission precluded the possibility of a straightforward major reduction in the size of the intermolecular vibrational basis (and therefore of the full product contracted basis) described above.

Other successful, and very challenging, applications of the methodology outlined above are the following: rigorous 8D quantum calculations of the intramolecular stretch fundamentals and frequency shifts of two H_2 molecules in the large clathrate hydrate cage [40], the fully coupled 9D quantum treatment of the intra- and intermolecular vibrational levels of H_2O in (rigid) C_{60} [41], and the fully coupled 9D quantum calculations of flexible H_2O/HDO intramolecular excitations and intermolecular states of the benzene-H_2O and benzene-HDO complexes (for rigid benzene), together with their IR and Raman spectra [42].

The bound state calculations of the hydrogen chloride–water dimer so far [20, 25] were performed for total angular momentum J=0. In this paper we present rigorous full-dimensional quantum calculations of the coupled intra- and intermolecular rovibrational states of the HH and DH isotopologues for total angular momentum J=1. As before [20, 25], the accurate 9D PIP-NN PES-2021 is employed. The J=1 rovibrational states are calculated using a slightly modified version of methodology used by us previously to compute in 9D the J=0, 1 rovibrational levels of H_2O/D_2O-CO[26] and HDO-CO [29]. The computed eigenstates encompass all intramolecular vibrational fundamentals of the dimers, together with the low-lying intermolecular rovibrational states within each intramolecular vibrational manifold. Particular attention is given to the dependence of the energies of the intermolecular rovibrational states on the (approximate) quantum number K, the projection of J on the intermolecular axis of the dimer, that is important for characterizing the nature of the rovibrational states.

II. COMPUTATIONAL METHODOLOGY

In a previous work on H_2O-CO and D_2O-CO [26], we presented a general method to compute the rovibrational levels of a water-diatom complex in full (9D) dimensionality. We make use of the same method in this study with only one significant modification pertaining

DOI:10.1063/1674-0068/cjcp2110189 ©2021 Chinese Physical Society

to the exploitation of nuclear-exchange symmetry, as described below in Sections II.C and II.E.

A. Rovibrational Hamiltonian and coordinates

The procedure starts with the rovibrational Hamiltonian of the water-hydrogen chloride dimer, as obtained from the general, weakly-bound-dimer expression presented by Brocks *et al.* [43]

$$\hat{H}(\mathbf{Q},\mathbf{q}_A,r_B,\Omega)=\hat{T}^{\rm rot}_{\rm inter}(\mathbf{Q},\Omega)+\hat{T}^A(\omega_A,\mathbf{q}_A)+\hat{T}^B(\omega_B,r_B)+V(\tilde{\mathbf{Q}},\mathbf{q}_A,r_B) \quad (1)$$

In Eq.(1), $\mathbf{Q}\equiv(r_0,\omega_A,\omega_B)$ denotes the collection of intermolecular coordinates: r_0 is the distance from the center of mass (c.m.) of the water moiety to that of the hydrogen-chloride moiety, $\omega_A\equiv(\alpha_A,\ \beta_A,\ \gamma_A)$ denotes the three Euler angles that fix the orientation of a cartesian frame attached to the water moiety (which we label BF_A) relative to one attached to the dimer (which we label DF), and $\omega_B\equiv(\alpha_B,\beta_B)$ denotes the two Euler angles that fix the orientation of the HCl internuclear vector ($\mathbf{r}_B$, which points from the Cl nucleus to the H nucleus) relative to DF. $\Omega\equiv(\alpha,\beta)$ denotes the Euler angles that orient the z axis of the DF frame ($\hat{z}_D$) relative to a space-fixed axis system (SF). $\mathbf{q}_A\equiv(R_1,R_2,\Theta)$ denotes the Radau coordinates [44–46] that we take as the water moiety's vibrational coordinates, and $r_B\equiv|\mathbf{r}_B|$ is the vibrational coordinate of the hydrogen-chloride moiety.

The origin of the DF frame is at the c.m. of the dimer, with $\hat{z}_D$ taken to be parallel to the vector ($\mathbf{r}_0$) pointing from the water c.m. to the hydrogen-chloride c.m. The BF_A (water-moiety) frame is centered at the water c.m. with axes defined by Radau, bisector-z embedding [47]: $\hat{z}_A$ is parallel to $\hat{R}_1+\hat{R}_2$ ($\hat{R}_i$ is the unit vector parallel to the $\mathbf{R}_i$ Radau vector), $\hat{y}_A$ is parallel to $\hat{R}_1\times\hat{R}_2$, and $\hat{x}_A=\hat{y}_A\times\hat{z}_A$.

$\hat{T}^{\rm rot}_{\rm inter}$, the rotational/intermolecular-kinetic-energy operator in Eq.(1), is given by [43]

$$\hat{T}^{\rm rot}_{\rm inter}(\mathbf{Q},\Omega)=-\frac{1}{2\mu_0}\frac{\partial^2}{\partial r_0^2}+B_0(r_0)(\hat{J}^2-\cot\beta\frac{\partial}{\partial\beta}-2\hat{\mathbf{J}}\cdot(\hat{\mathbf{j}}_A+\hat{\mathbf{j}}_B)+\hat{j}_A^2+\hat{j}_B^2+2\hat{\mathbf{j}}_A\cdot\hat{\mathbf{j}}_B) \quad (2)$$

where μ_0 is the dimer's reduced mass, $B_0(r_0)\equiv1/(2\mu_0 r_0^2)$, $\hat{\mathbf{J}}$ is the vector operator corresponding to the rotational angular momentum of the dimer measured with respect to the DF frame, and $\mathbf{j}_A$ and $\mathbf{j}_B$ are the vector operators corresponding, respectively, to the rotational angular momenta of the water and hydrogen-chloride moieties measured with respect to the DF frame.

$\hat{T}^A$ and $\hat{T}^B$, the rotation-vibration kinetic-energy operators of the water and hydrogen-chloride monomers, respectively, can be expressed as

$$\hat{T}^A(\omega_A,\mathbf{q}_A)\equiv\hat{T}^A_v(\mathbf{q}_A)+\hat{T}^A_r(\omega_A,\mathbf{q}_A)+\hat{T}^A_{\rm cor}(\omega_A,\mathbf{q}_A) \quad (3)$$

with $\hat{T}^A_r$, $\hat{T}^A_v$, and $\hat{T}^A_{\rm cor}$ given respectively by Eqs.(4), (5), and (6) of Ref.[26] (as adapted from Ref.[47]), and

$$\hat{T}^B(\omega_B,r_B)\equiv\hat{T}^B_v(r_B)+\hat{T}^B_r(\omega_B,r_B) \quad (4)$$

with $\hat{T}^B_r$ and $\hat{T}^B_v$ given, respectively, by Eq.(9) and Eq.(10) of Ref.[26].

Finally, $V(\mathbf{Q},\mathbf{q}_A,r_B)$, the 9D potential-energy function in Eq.(1), is taken to be the water-hydrogen chloride potential PES-2021 from Ref.[20]. Note that the dimer potential is independent of the individual values of α_A and α_B and is dependent only on their difference $\tilde{\alpha}\equiv\alpha_A-\alpha_B$ (*e.g.*, see Appendix B of Ref.[39]). We denote this dependence by defining the five "reduced" intermolecular coordinates $\tilde{\mathbf{Q}}\equiv(r_0,\tilde{\alpha},\beta_A,\gamma_A,\beta_B)$. One sees that V is a function of nine coordinates, as expected for the PES associated with a five-atom system.

B. General approach to computing the eigenstates of $\hat{H}$

In order to solve for the eigenstates of $\hat{H}$ we first divide it into four terms, three reduced-dimension Hamiltonians and a remainder term:

$$\hat{H}=\hat{H}^{\rm rot}_{\rm inter}(\mathbf{Q},\Omega)+\hat{H}^A_v(\mathbf{q}_A)+\hat{H}^B_v(r_B)+\Delta\hat{H}(\mathbf{Q},\mathbf{q}_A,r_B) \quad (5)$$

DOI:10.1063/1674-0068/cjcp2110189 ©2021 Chinese Physical Society

In this equation the "rotational-intermolecular Hamiltonian" is defined as

$$\hat{H}^{\rm rot}_{\rm inter} \equiv \hat{T}^{\rm rot}_{\rm inter}(\mathbf{Q},\Omega) + \hat{T}^{A}_{r}(\omega_A,\mathbf{q}^0_A) + \hat{T}^{B}_{r}(\omega_B,r^0_B) + V_{\rm inter}(\tilde{\mathbf{Q}}) \quad (6)$$

where $\mathbf{q}^0_A=(R^0_1,R^0_2,\Theta^0)$ represents fixed values for the three vibrational coordinates of the water moiety, r^0_B is a fixed value for the hydrogen-chloride vibrational coordinate, and

$$V_{\rm inter}(\tilde{\mathbf{Q}}) \equiv V(\tilde{\mathbf{Q}},\mathbf{q}^0_A,r^0_B) \quad (7)$$

The vibrational Hamiltonian for the water moiety is defined as

$$\hat{H}^{A}_{v}(\mathbf{q}_A) \equiv \hat{T}^{A}_{v}(\mathbf{q}_A) + V^{A}(\mathbf{q}_A) \quad (8)$$

where

$$V^{A}(\mathbf{q}_A) \equiv V(\tilde{\mathbf{Q}}^{\infty},\mathbf{q}_A,r^0_B) \quad (9)$$

and $\tilde{\mathbf{Q}}^{\infty}$ denotes fixed values of the reduced intermolecular coordinates corresponding to a large value of the inter-monomer distance (more on this in Section II.D). $\hat{H}^{B}_{v}$, the vibrational Hamiltonian for the hydrogen-chloride moiety, is defined as

$$\hat{H}^{B}_{v}(r_B) = \hat{T}^{B}_{v}(r_B) + V^{B}(r_B) \quad (10)$$

where

$$V^{B}(r_B) \equiv V(\tilde{\mathbf{Q}}^{0},\mathbf{q}^0_A,r_B) \quad (11)$$

and $\tilde{\mathbf{Q}}^0$ denotes fixed values of the reduced intermolecular coordinates (more on this in Section II.D). Finally, the remainder term in Eq.(5) is given by

$$\begin{aligned}&\Delta\hat{H}(\mathbf{Q},\mathbf{q}_A,r_B)\\ =\ &[\hat{T}^{A}_{r}(\omega_A,\mathbf{q}_A)-\hat{T}^{A}_{r}(\omega_A,\mathbf{q}^0_A)]+\hat{T}^{A}_{\rm cor}(\omega_A,\mathbf{q}_A)\\ &+[\hat{T}^{B}_{r}(\omega_B,r_B)-\hat{T}^{B}_{r}(\omega_B,r^0_B)]+\Delta V(\tilde{\mathbf{Q}},\mathbf{q}_A,r_B)\end{aligned} \quad (12)$$

where

$$\Delta V(\tilde{\mathbf{Q}},\mathbf{q}_A,r_B) \equiv V(\tilde{\mathbf{Q}},\mathbf{q}_A,r_B) - V_{\rm inter}(\tilde{\mathbf{Q}}) - V^{A}(\mathbf{q}_A) - V^{B}(r_B) \quad (13)$$

Second, we solve for the lowest-energy eigenstates of the reduced Hamiltonians $\hat{H}^{\rm rot}_{\rm inter}$, $\hat{H}^{A}_{v}$, and $\hat{H}^{B}_{v}$. We denote the set of such eigenstates of $\hat{H}^{\rm rot}_{\rm inter}$ for a particular value of the rotational angular-momentum quantum number J as $|\kappa,J\rangle$, κ=1, ..., $N_{\rm inter}$. Those corresponding to $\hat{H}^{A}_{v}$ we denote as $|\mathbf{v}_A\rangle$, where $\mathbf{v}_A\equiv(v_1,v_2,v_3)$ represents the set of three quantum numbers (symmetric-stretch, bend, asymmetric-stretch) specifying the water-moiety vibrational state. And, we denote those corresponding to $\hat{H}^{B}_{v}$ as $|v_B\rangle$, where v_B is the HCl vibrational quantum number.

Finally, we construct a set of 9D basis states for a given value of J consisting of products of the form

$$|\kappa,J;\mathbf{v}_A;v_B\rangle \equiv |\kappa,J\rangle|\mathbf{v}_A\rangle|v_B\rangle \quad (14)$$

and diagonalize the matrix of $\hat{H}$ expressed in this basis. Since the matrix elements of $\hat{H}^{\rm rot}_{\rm inter}$, $\hat{H}^{A}_{v}$, and $\hat{H}^{B}_{v}$ in this basis are trivially obtained, the major effort in solving for the eigenstates of $\hat{H}$ involves the computation of the matrix elements of $\Delta\hat{H}$.

C. Calculation of the J=1 eigenstates of $\hat{H}^{\rm rot}_{\rm inter}$

The procedure used here to calculate the J=1 eigenstates of $\hat{H}^{\rm rot}_{\rm inter}$ is largely the same as that outlined in Sec.2.2 of Ref.[25]. That is, we employ the Chebyshev version of filter diagonalization to diagonalize matrices of the operator in symmetry-specific bases constructed from the primitive basis functions [48]

$$|s,j_A,k_A,m,j_B;JK\rangle \equiv |r_{0,s}\rangle|j_A,k_A,m\rangle|j_B,K-m\rangle|JK\rangle \quad (15)$$

with J=1 and K=−1, 0, 1. In Eq.(15), $|r_{0,s}\rangle$ denotes one of 20 functions associated with a potential-optimized discrete variable representation (PODVR) [49, 50] covering the r_0 coordinate (for details see Sec.3.1.2 of Ref.[20]), $|j_A,k_A,m\rangle$ (j_A=0, ···, 10), denotes a symmetric-top eigenfunction covering the ω_A coordinates, $|j_B,K-m\rangle$ (j_B=0, ···, 18) denotes a spherical harmonic function covering the ω_B coordinates, and $|JK\rangle$ is a normalized "little-d" Wigner matrix element

$$|JK\rangle \equiv \sqrt{\frac{2J+1}{2}}d^{J}_{0,K}(\beta) \quad (16)$$

As in Ref.[25], we choose the $\mathbf{q}^0_A$ and r^0_B values required to obtain $V_{\rm inter}$ (see Eq.(7)) so as to correspond, respectively, to a water moiety with OH bond distances of 0.96 Å and a bond angle of 104.52°, and a hydrogen chloride moiety with a bond distance of 1.3097 Å. This rigid-water geometry is very close to the equilibrium geometry of the free monomer [51]. The HCl bond distance is slightly longer than the expectation value of the computed ground state of $\hat{H}^{B}_{v}$.

The only substantive difference in this work from that

DOI:10.1063/1674-0068/cjcp2110189 ©2021 Chinese Physical Society

of Sec.2.2 of Ref.[25] is that here we make full use of the G_4 symmetry of the HH and DH dimers to block-diagonalize the $\hat{H}^{\rm rot}_{\rm inter}$ matrix for a given species into four blocks. That is, in addition to symmetrizing the basis functions with respect to inversion (as in Ref.[25]), we also symmetrize them with respect to exchange of the H nuclei of the water. The former was accomplished by using Eq.(31) of Ref.[25] to obtain a random state function of definite parity with which to initiate the filter-diagonalization procedure. The latter was accomplished by including the functions in Eq.(15) with only even or only odd values of k_A in that random initial state function. As a result, for each isotopologue four different filter-diagonalization runs—one for each G_4 irreducible representation ("irrep")—were carried out to obtain all the $|\kappa,\ J\rangle$. For the *para* (k_A even)/*ortho* (k_A odd) runs a total of 793,700/784,800 functions in Eq.(15) contributed to the basis. The number of independent basis functions associated with a given irrep block is about a factor of two smaller than these numbers due to the parity-filtering employed to produce the initial state function for that block.

D. Calculation of the eigenstates of $\hat{H}^A_v$ and $\hat{H}^B_v$

The eigenstates of $\hat{H}^A_v$ and $\hat{H}^B_v$ were computed in this work in a manner identical to the procedures employed in Ref.[25]. As such, we refer the reader to that work for details. Here, we simply point out that the $\tilde{\mathbf{Q}}^\infty$-coordinate values used to obtain V^A (see Eq.(9)) were chosen to be those associated with the planar, C_{2v} dimer geometry with r_0=26.5 Å. Thus, the computed $|\mathbf{v}_A\rangle$ are essentially isolated-water vibrational states. In contrast, the $\tilde{\mathbf{Q}}^0$-coordinate values required to obtain V^B (see Eq.(11)) were chosen to be the expectation values of the $\tilde{\mathbf{Q}}$ for the ground state of $\hat{H}^{\rm rot}_{\rm inter}$ for J=0. Hence, the eigenstates of $\hat{H}^B_v$ are those corresponding to a "dimer-adapted" HCl (DCl) potential. We made this choice for the hydrogen-chloride moiety because of the information from experiment indicating a significant perturbation of that moiety upon dimerization with water [5, 7].

E. Calculation of the eigenstates of $\hat{H}$

The J=1 eigenstates of $\hat{H}$ were computed in this work by a procedure almost identical to that described in Sec.II E of Ref.[26]. The only substantive procedural difference from the latter work is that here we fully block-diagonalize the $\hat{H}$ matrix into the four blocks associated with the G_4 irreps, whereas in Ref.[26] we limited the block diagonalization to just two parity-specific blocks and thus neglected to use all of the *ortho/para* symmetry information available. We chose to make fuller use of symmetry in this work owing to the considerably larger 9D basis sets that we employ here relative to those used previously.

Explicit incorporation of *ortho/para* symmetry into the 9D basis is somewhat more involved than incorporating parity into that basis. The parity of the 9D basis function $|\kappa, J; \mathbf{v}_A; v_B\rangle$ is entirely determined by the parity of the intermolecular eigenstate $|\kappa, J\rangle$. Hence, to obtain even- (odd-) parity eigenfunctions of $\hat{H}$ one simply includes only even- (odd-) parity $|\kappa,\ J\rangle$ in constructing one's 9D basis. In contrast, the symmetry of a 9D basis function with respect to H exchange is determined by the way in which both $|\kappa,\ J\rangle$ and $|\mathbf{v}_A\rangle$ transform upon H exchange. Denoting the exchange operation as (12), then

$$\begin{aligned}(12)|\kappa, J; \mathbf{v}_A; v_B\rangle &= (12)|\kappa, J\rangle \times (12)|\mathbf{v}_A\rangle \times |v_B\rangle \\ &= \sigma_{\kappa,J}\sigma_{\mathbf{v}_A}|\kappa, J; \mathbf{v}_A; v_B\rangle \end{aligned} \tag{17}$$

where $\sigma_{\kappa,J}$=±1 and $\sigma_{\mathbf{v}_A}$=±1 are, respectively, the eigenvalues of $|\kappa, J\rangle$ and $|\mathbf{v}_A\rangle$ with respect to the (12) operator. Thus, both *ortho* and *para* $|\kappa,\ J\rangle$ states contribute to the same symmetry block of the $\hat{H}$ matrix, as do both *ortho* and *para* $|\mathbf{v}_A\rangle$ states.

With the above in mind, we now outline the calculation and diagonalization of the symmetry-specific $\hat{H}$ matrices. We start with a set of parity-specific 9D basis functions containing both *ortho* and *para* members. We proceed to compute, per Sections II E 1−3 of Ref.[26], the matrix elements of $\Delta\hat{H}$ in the set of states $|\kappa,\ J;\ \eta;\ \xi\rangle$, where $|\eta\rangle$ and $|\xi\rangle$ denote the DVR basis functions that contribute to the eigenstates of $\hat{H}^A_v$ and $\hat{H}^B_v$, respectively. We then calculate the matrix elements of $\hat{H}$,

$$\begin{aligned}&\langle\kappa', J; \mathbf{v}'_A; v'_B|\hat{H}|\kappa, J; \mathbf{v}_A; v_B\rangle \\ =\ & (E_{\kappa,J} + E_{\mathbf{v}_A} + E_{v_B})\delta_{\kappa'\kappa}\delta_{\mathbf{v}'_A\mathbf{v}_A}\delta_{v'_Bv_B} \\ &+ \sum_{\eta,\eta',\xi}\Big(\langle\mathbf{v}'_A|\eta'\rangle\langle\eta|\mathbf{v}_A\rangle\langle v'_B|\xi\rangle\langle\xi|v_B\rangle \\ &\qquad \langle\kappa', J; \eta'; \xi|\Delta\hat{H}|\kappa, J; \eta; \xi\rangle\Big)\end{aligned} \tag{18}$$

for the *para* 9D basis states and diagonalize that matrix by direct diagonalization. ($E_{\kappa,J}$, $E_{\mathbf{v}_A}$, and E_{v_B} are the eigenvalues of $|\kappa, J; \mathbf{v}_A; v_b\rangle$ with respect to $\hat{H}^{\rm rot}_{\rm inter}$,

DOI:10.1063/1674-0068/cjcp2110189 ©2021 Chinese Physical Society

$\hat{H}_v^A$, and $\hat{H}_v^B$, respectively.) We repeat the evaluation of Eq.(18) and subsequent matrix diagonalization for the *ortho* basis states. In this way both the *para* and *ortho* eigenstates of a given parity are obtained. A separate calculation of the same type, but starting with basis states of opposite parity, yields the remainder of the 9D eigenstates.

In constructing the 9D basis sets for each isotopologue we included the 21 lowest-energy eigenstates of $\hat{H}_v^A$ and the 5 lowest-energy eigenstates of $\hat{H}_v^B$, just as in the J=0 calculations of Ref.[25]. As for the $|\kappa, J\rangle$, we included for each parity the 140 lowest-energy *para* and the 140 lowest-energy *ortho* states. For the HH species this amounted to all the eigenstates of $\hat{H}_{\rm inter}^{\rm rot}$ up to ∼920 cm^{-1} above the ground state. For DH all the $\hat{H}_{\rm inter}^{\rm rot}$ eigenstates up to about 850 cm^{-1} above the $\hat{H}_{\rm inter}^{\rm rot}$ ground state were included. In all cases (for both isotopologues and for each G_4-irrep block of the $\hat{H}$ matrix) the total number of basis states corresponding to each block thus amounted to 14,700.

III. RESULTS AND DISCUSSION

Selected low-energy J=1, K=0 and J=1, K=1 intermolecular states of the HH and DH isotopologues from the 9D calculations, for the monomers in their ground vibrational states, are presented in Tables I and II, respectively. Their assignments in terms of the fundamentals, overtones, and combinations of three intermolecular modes, $\nu_{\rm inversion}$, $\nu_{\rm stretch}$, and $\nu_{\rm rock}$, are explained in Ref.[20]. It is evident that the K=1 intermolecular states are closely spaced doublets (to within a fraction of a wavenumber) and, strictly speaking, the label K stands for the absolute value $|K|$. Comparison of the J=1, K=0 states of the HH and DH dimers in Tables I and II, respectively, with the corresponding J=0 states of the two isotopologues (Table I in Ref.[25]) shows that they differ in energy by at most 0.5 cm^{-1}.

The same 9D J=1, K=0 and J=1, K = 1 intermolecular states, but now in the ν_2, $\nu_{\rm HCl}$ ($\nu_{\rm DCl}$), ν_1 and ν_3 intramolecular vibrational manifolds, respectively, are shown in Tables III−VI for the HH dimer and in Tables VII−X for the DH dimer. In all instances, the energy differences between J=1, K=0 states reported here and the corresponding previously calculated J=0 states (Tables VII and VIII in Ref.[25]) do not exceed 0.5 cm^{-1}. This means that the observations made earlier [20, 25] regarding the significant effects of the intramolecular vibrational excitations of the monomers on the J=0 in-

TABLE I Low-energy J=1 intermolecular rovibrational states of the HH dimer in the manifold of the intramolecular vibrational ground state from 9D calculations.

Intermolecular state	$\|K\|$	ΔE[a]	irrep	BSN
Ground state	0	0.000	$A_{\rm u}$	0.9927
	1	13.736	$B_{\rm u}$	0.9925
	1	13.740	$B_{\rm g}$	0.9925
$\nu_{\rm inversion}$	0	85.444	$B_{\rm g}$	0.9931
	1	94.653	$A_{\rm g}$	0.9923
	1	94.794	$A_{\rm u}$	0.9924
$\nu_{\rm stretch}$	0	131.817	$A_{\rm u}$	0.9855
	1	145.586	$B_{\rm u}$	0.9792
	1	145.590	$B_{\rm g}$	0.9852
$\nu_{\rm rock}$	0	145.893	$B_{\rm u}$	0.9883
	1	164.269	$A_{\rm g}$	0.9932
	1	164.481	$A_{\rm u}$	0.9933
$2\nu_{\rm inversion}$	0	217.157	$A_{\rm u}$	0.9919
	1	222.299	$B_{\rm u}$	0.9925
	1	222.322	$B_{\rm g}$	0.9925
$\nu_{\rm inversion} + \nu_{\rm stretch}$	0	217.534	$B_{\rm g}$	0.9853
	1	226.469	$A_{\rm g}$	0.9849
	1	226.612	$A_{\rm u}$	0.9849

[a] ΔE is a state's energy in cm^{-1} relative to that of the J=1 ground state of the dimer.

TABLE II Low-energy J=1 intermolecular rovibrational states of the DH dimer in the manifold of the intramolecular vibrational ground state from 9D calculations.

Intermolecular state	$\|K\|$	ΔE[a]	irrep	BSN
Ground state	0	0.000	$A_{\rm u}$	0.9949
	1	13.732	$B_{\rm u}$	0.9948
	1	13.734	$B_{\rm g}$	0.9948
$\nu_{\rm inversion}$	0	84.043	$B_{\rm g}$	0.9957
	1	92.882	$A_{\rm g}$	0.9953
	1	92.924	$A_{\rm u}$	0.9954
$\nu_{\rm stretch}$	0	133.374	$A_{\rm u}$	0.9917
	1	147.154	$B_{\rm u}$	0.9915
	1	147.162	$B_{\rm g}$	0.9915
$\nu_{\rm rock}$	0	138.753	$B_{\rm u}$	0.9956
	1	156.099	$A_{\rm g}$	0.9950
	1	156.139	$A_{\rm u}$	0.9950
$2\nu_{\rm inversion}$	0	212.783	$A_{\rm u}$	0.9952
	1	215.930	$B_{\rm u}$	0.9955
	1	215.931	$B_{\rm g}$	0.9955
$\nu_{\rm inversion} + \nu_{\rm stretch}$	0	217.712	$B_{\rm g}$	0.9924
	1	226.339	$A_{\rm g}$	0.9921
	1	226.430	$A_{\rm u}$	0.9922

[a] ΔE is a state's energy in cm^{-1} relative to that of the J=1 ground state of the dimer.

DOI:10.1063/1674-0068/cjcp2110189 ©2021 Chinese Physical Society

TABLE III Low-energy J=1 intermolecular rovibrational states of the HH dimer in the ν_2 intramolecular vibrational manifold from 9D calculations.

Intermolecular state	$\|K\|$	ΔE^a/cm^{-1}	irrep	BSN
Ground state	0	0.000	A_u	0.9872
	1	13.847	B_u	0.9868
	1	13.850	B_g	0.9868
$\nu_{inversion}$	0	93.492	B_g	0.9897
	1	102.281	A_g	0.9896
	1	102.388	A_u	0.9897
$\nu_{stretch}$	0	131.478	A_u	0.9799
	1	145.359	B_u	0.9782
	1	145.363	B_g	0.9795
ν_{rock}	0	147.216	B_u	0.9884
	1	166.083	A_g	0.9892
	1	166.228	A_u	0.9894
$2\nu_{inversion}$	0	232.477	A_u	0.9867
	1	236.952	B_u	0.9869
	1	236.968	B_g	0.9869
$\nu_{inversion}+\nu_{stretch}$	0	225.216	B_g	0.9815
	1	233.680	A_g	0.9815
	1	233.817	A_u	0.9816

[a] ΔE is a state's energy relative to that of the lowest-energy J=1 state in the ν_2 manifold. The latter is at an energy of 1595.782 cm^{-1} relative to the J=1 ground state of the dimer.

TABLE IV Low-energy J=1 intermolecular rovibrational states of the HH dimer in the ν_{HCl} intramolecular vibrational manifold from 9D calculations.

Intermolecular state	$\|K\|$	ΔE^a/cm^{-1}	irrep	BSN
Ground state	0	0.000	A_u	0.9089
	1	13.278	B_u	0.9075
	1	13.280	B_g	0.9074
$\nu_{inversion}$	0	68.983	B_g	0.8988
	1	79.192	A_g	0.8883
	1	79.550	A_u	0.8893
$\nu_{stretch}$	0	137.036	A_u	0.7718
	1	150.446	B_u	0.7677
	1	150.456	B_g	0.7683
ν_{rock}	0	164.334	B_u	0.9315
	1	180.916	A_g	0.9158
	1	181.315	A_u	0.9165
$2\nu_{inversion}$	0	211.205	A_u	0.8859
	1	218.149	B_u	0.8841
	1	218.187	B_g	0.8839
$\nu_{inversion}+\nu_{stretch}$	0	209.306	B_g	0.7542
	1	219.212	A_g	0.7464
	1	219.887	A_u	0.7495

[a] ΔE is a state's energy relative to that of the lowest-energy J=1 state in the ν_{HCl} manifold. The latter is at an energy of 2727.674 cm^{-1} relative to the J=1 ground state of the dimer.

termolecular vibrational eigen states of these dimers apply also to the J=1, K=0 intermolecular states in this work.

While the energies of the J=1, K=0 intermolecular states of the HH and DH dimers are very close to those of their J=0 counterparts, a glance at Tables I-X shows that in all cases the K=1 state is 5 to 19 cm^{-1} higher in energy than the corresponding J=1,K=0 state. The $E_{J=1,|K|=1}-E_{J=1,K=0}$ energy differences for selected low-energy intermolecular states in the manifolds of the intramolecular vibrational fundamentals are summarized in Table XI for the HH dimer and in Table XII for the DH dimer. $E_{J=1,|K|=1}$ is taken to be the average of energies of the nearly degenerate pair of $|K|$=1 states. For the HH dimer in ground intramolecular state, $E_{J=1,|K|=1}-E_{J=1,K=0}$ is equal to 13.74 cm^{-1} for the ground intermolecular state, 9.28 cm^{-1} for the inversion fundamental $\nu_{inversion}$, 5.16 cm^{-1} for the inversion overtone $2\nu_{inversion}$, 18.48 cm^{-1} for the rock fundamental ν_{rock}, and 13.77 cm^{-1} for the stretch fundamental $\nu_{stretch}$. The analogous results in Table XII for the DH dimer are very similar.

These significant variations of $E_{J=1,|K|=1}-E_{J=1,K=0}$ with the intermolecular vibrational states can be rationalized as follows, starting with those for the inversion mode. The positions of the H atoms of H_2O largely determine the magnitude of the A rotational constant and thus $E_{J=1,|K|=1}-E_{J=1,K=0}$. In our treatment [20], the deviation of the H_2O moiety from the planar C_{2V} geometry of the complex is described by β_A, the water polar angle between the C_2 axis of H_2O and the vector connecting the c.m. of H_2O to that of HCl. The expectation value of β_A, and therefore the non-planarity of the complex, increases markedly (relative to the ground-state value) for $\nu_{inversion}$, and even more for $2\nu_{inversion}$ [20]. This results in the decrease of the A rotational constant, and hence $E_{J=1,|K|=1}-E_{J=1,K=0}$, in going from the intermolecular ground state to $\nu_{inversion}$ and $2\nu_{inversion}$. Exciting ν_{rock} also increases β_A, but much less than $\nu_{inversion}$ [20]. Moreover, this increase in β_A occurs roughly within O−HCl plane [20]. Apparently, this brings the H atoms of water closer (on the average)

DOI:10.1063/1674-0068/cjcp2110189 ©2021 Chinese Physical Society

TABLE V Low-energy J=1 intermolecular rovibrational states of the HH dimer in the ν_1 intramolecular vibrational manifold from 9D calculations.

Intermolecular state	$\|K\|$	ΔE[a]	irrep	BSN
Ground state	0	0.000	A_u	0.9864
	1	13.440	B_u	0.9728
	1	13.444	B_g	0.9724
$\nu_{inversion}$	0	78.764	B_g	0.9857
	1	88.030	A_g	0.9803
	1	88.173	A_u	0.9849
$\nu_{stretch}$	0	132.027	A_u	0.9755
	1	145.510	B_u	0.9741
	1	145.513	B_g	0.9744
ν_{rock}	0	144.305	B_u	0.9881
	1	162.071	A_g	0.9836
	1	162.279	A_u	0.9768
$2\nu_{inversion}$	0	207.483	A_u	0.9797
	1	212.957	B_u	0.9586
	1	212.980	B_g	0.9637
$\nu_{inversion}+\nu_{stretch}$	0	211.588	B_g	0.9743
	1	220.632	A_g	0.8727
	1	220.724	A_u	0.8643

[a] ΔE is a state's energy in cm^{-1} relative to that of the lowest-energy J=1 state in the ν_1 manifold. The latter is at an energy of 3649.966 cm^{-1} relative to the J=1 ground state of the dimer.

TABLE VI Low-energy J=1 intermolecular rovibrational states of the HH dimer in the ν_3 intramolecular vibrational manifold from 9D calculations.

Intermolecular state	$\|K\|$	ΔE[a]	irrep	BSN
Ground state	0	0.000	B_u	0.9880
	1	13.584	A_u	0.9837
	1	13.588	A_g	0.9831
$\nu_{inversion}$	0	77.050	A_g	0.9871
	1	86.329	B_g	0.9845
	1	86.474	B_u	0.9848
$\nu_{stretch}$	0	131.514	B_u	0.9785
	1	145.099	A_g	0.3411
	1	145.154	A_g	0.6360
	1	145.131	A_u	0.9754
ν_{rock}	0	143.530	A_u	0.9815
	1	161.817	B_g	0.9296
	1	162.006	B_u	0.8993
$2\nu_{inversion}$	0	204.195	B_u	0.9827
	1	209.657	A_u	0.9827
	1	209.681	A_g	0.9807
$\nu_{inversion}+\nu_{stretch}$	0	209.338	A_g	0.9779
	1	218.369	B_g	0.9696
	1	218.515	B_u	0.9373

[a] ΔE is a state's energy in cm^{-1} relative to that of the lowest-energy J=1 state in the ν_3 manifold. The latter is at an energy of 3749.848 cm^{-1} relative to the J=1 ground state of the dimer.

to the O−Cl heavy-atom axis, thereby increasing the A rotational constant and $E_{J=1,|K|=1}-E_{J=1,K=0}$.

The above also explains why for a given intermolecular state of either HH or DH dimer, the variation of $E_{J=1,|K|=1}-E_{J=1,K=0}$ (relative to value in the ground intramolecular state) for different intramolecular vibrational states is much weaker.

Finally, we discuss briefly the last column in Tables I−X labeled BSN, for basis-set norm. The entries in this column measure the contribution of the dominant product inter/intra-basis state to the given 9D eigenstate. For the majority of states shown, the BSN is close to 1, meaning that these eigenstates are highly "pure", *i.e.*, dominated by a single inter/intra-basis state. But there are some exceptions. For many of the states in Tables IV and VIII, belonging to the ν_{HCl} and ν_{DCl} intramolecular vibrational manifolds, respectively, the BSNs are considerably smaller than 1, as low as 0.6−0.7, indicating rather strong basis-state mixing. This was already noted for the J=0 states of the HH dimer [20], and is consistent with the observation that the ν_{HCl} and ν_{DCl} modes couple most strongly to the intermolecular vibrational modes of the dimers [20, 25].

Small BSNs can also arise from the coupling between K=1 intermolecular vibrational states belonging to two different intramolecular vibrational manifolds. We have two examples of this. In Table VI, in the ν_3 intramolecular vibrational manifold of the HH dimer, two K=1 $\nu_{stretch}$ states of A_g symmetry arise from such a coupling, leading to a splitting of the "pure" K=1 state and small BSNs. In addition, in Table IX, for the DH dimer, the same type of coupling splits both members of the $|K|$=1 doublet of the ground intermolecular state in the ν_1 intramolecular vibrational manifold.

The energies of the J=1 intramolecular vibrational levels of the HH and DH dimer from the 9D calculations differ negligibly from those of their J=0 counterparts reported previously [20, 25]. Therefore, the detailed discussion in Refs.[20] and [25] regarding the J=0 intramolecular vibrational eigenstates and their frequency shifts relative to the isolated monomer values applies

DOI:10.1063/1674-0068/cjcp2110189 ©2021 Chinese Physical Society

TABLE VII Low-energy J=1 intermolecular rovibrational states of the DH dimer in the ν_2 intramolecular vibrational manifold from 9D calculations.

Intermolecular state	$\|K\|$	ΔE^a/cm^{-1}	irrep	BSN
Ground state	0	0.000	A_u	0.9872
	1	13.813	B_u	0.9869
	1	13.814	B_g	0.9869
$\nu_{inversion}$	0	92.374	B_g	0.9909
	1	100.638	A_g	0.9905
	1	100.663	A_u	0.9906
$\nu_{stretch}$	0	133.082	A_u	0.9830
	1	146.941	B_u	0.9827
	1	146.949	B_g	0.9828
ν_{rock}	0	139.991	B_u	0.9889
	1	157.971	A_g	0.9884
	1	157.987	A_u	0.9885
$2\nu_{inversion}$	0	227.405	A_u	0.9873
	1	229.533	B_g	0.9850
	1	229.534	B_u	0.9850
$\nu_{inversion}+\nu_{stretch}$	0	225.578	B_g	0.9869
	1	233.593	A_g	0.9864
	1	233.676	A_u	0.9865

[a] ΔE is a state's energy relative to that of the lowest-energy J=1 state in the ν_2 manifold. The latter is at an energy of 1594.967 cm^{-1} relative to the J=1 ground state of the dimer.

TABLE VIII Low-energy J=1 intermolecular rovibrational states of the DH dimer in the ν_{DCl} intramolecular vibrational manifold from 9D calculations.

Intermolecular state	$\|K\|$	ΔE^a/cm^{-1}	irrep	BSN
Ground state	0	0.000	A_u	0.6447
	1	14.826	B_u	0.7738
	1	14.835	B_g	0.7718
$\nu_{inversion}$	0	72.700	B_g	0.9333
	1	82.682	A_g	0.8992
	1	82.757	A_u	0.8997
$\nu_{stretch}$	0	137.681	A_u	0.5852
	1	151.047	B_u	0.7254
	1	151.055	B_g	0.7273
ν_{rock}	0	150.407	B_u	0.7886
	1	167.059	A_g	0.9346
	1	167.126	A_u	0.9347
$2\nu_{inversion}$	0	208.865	A_u	0.9021
	1	212.907	B_u	0.5317
	1	212.955	B_g	0.5657
$\nu_{inversion}+\nu_{stretch}$	0	211.162	B_g	0.8357
	1	220.687	A_g	0.8058
	1	220.942	A_u	0.8095

[a] ΔE is a state's energy relative to that of the lowest-energy J=1 state in the ν_{DCl} manifold. The latter is at an energy of 1977.511 cm^{-1} relative to the J=1 ground state of the dimer.

without any changes to the J=1 intramolecular eigenstates in this work.

We take the opportunity to discuss here one aspect of these results that was not addressed previously [20, 25], the fractional vibrational frequency shift (redshift) of the HCl and DCl stretch fundamentals in the HH and DH dimers, respectively. This quantity is defined as $\Delta\nu/\nu_{free}$, where $\Delta\nu$ is the HCl/DCl stretch frequency shift in the dimers, while ν_{free} is the isolated HCl/DCl stretch frequency. From our 9D calculations for the HH dimer [20], $\Delta\nu_{HCl}$=−157.92 cm^{-1}, and $\nu_{HCl_{free}}$=2885.26 cm^{-1}. Consequently, $\Delta\nu_{HCl}/\nu_{HCl_{free}}$=−0.055. Likewise, for the DH dimer, from the 9D calculations [25], $\Delta\nu_{DCl}$=−112.82 cm^{-1}, and $\nu_{DCl_{free}}$=2090.36 cm^{-1}. Therefore, $\Delta\nu_{DCl}/\nu_{DCl_{free}}$=−0.054. Thus, the two fractional vibrational frequency shifts $\Delta\nu_{HCl}/\nu_{HCl_{free}}$ and $\Delta\nu_{DCl}/\nu_{DCl_{free}}$ are nearly identical, remarkably unaffected by the H/D isotopic subsitution. This is consistent with the prediction of the simple theory due to Buckingham, based on the first- and second-order perturbation theory, of the effects of solvent molecules on the intramolecular stretch frequency of a solute diatomic molecule [52, 53].

IV. CONCLUSION

We have presented the results of the full-dimensional and fully coupled quantum calculations of the intra- and intermolecular rovibrational states of the HH and DH dimers for total angular momentum J=1. This extends our recent rigorous studies of the J=0 9D coupled inter- and intramolecular vibrational eigenstates of these two dimers, as well as two other H/D isotopologues of the hydrogen chloride-water dimer [20, 25]. The accurate 9D PIP-NN PES-2021 developed in Ref.[20] is employed in this work, together with the slight modification of the sophisticated and highly efficient bound-state methodology that we used earlier to compute the 9D J=0, 1 rovibrational states of H_2O/D_2O−CO [26] and HDO–CO [29].

The results include all intramolecular vibrational fundamentals of the dimers, in combination with the low-

DOI:10.1063/1674-0068/cjcp2110189 ©2021 Chinese Physical Society

TABLE IX Low-energy J=1 intermolecular rovibrational states of the DH dimer in the ν_1 intramolecular vibrational manifold from 9D calculations.

Intermolecular state	$\|K\|$	ΔE[a]	irrep	BSN
Ground state	0	0.000	A_u	0.9737
	1	13.070	B_u	0.2938
	1	13.543	B_u	0.6936
	1	13.076	B_g	0.3012
	1	13.548	B_g	0.6863
$\nu_{inversion}$	0	77.074	B_g	0.9898
	1	86.060	A_g	0.9813
	1	86.103	A_u	0.9813
$\nu_{stretch}$	0	133.497	A_u	0.9750
	1	147.214	B_u	0.7405
	1	147.221	B_g	0.7394
ν_{rock}	0	137.411	B_u	0.9771
	1	154.071	A_g	0.9768
	1	154.118	A_u	0.9420
$2\nu_{inversion}$	0	203.208	A_u	0.9806
	1	206.895	B_u	0.9772
	1	206.898	B_g	0.9770
$\nu_{inversion}+\nu_{stretch}$	0	211.491	B_g	0.9570
	1	220.260	A_g	0.9716
	1	220.358	A_u	0.9718

[a] ΔE is a state's energy in cm^{-1} relative to that of the lowest-energy J=1 state in the ν_1 manifold. The latter is at an energy of 3650.458 cm^{-1} relative to the J=1 ground state of the dimer.

TABLE X Low-energy J=1 intermolecular rovibrational states of the DH dimer in the ν_3 intramolecular vibrational manifold from 9D calculations.

Intermolecular state	$\|K\|$	ΔE[a]	irrep	BSN
Ground state	0	0.000	B_u	0.9902
	1	13.580	A_u	0.9898
	1	13.582	A_g	0.9898
$\nu_{inversion}$	0	75.600	A_g	0.9853
	1	84.617	B_g	0.9719
	1	84.658	B_u	0.9727
$\nu_{stretch}$	0	133.026	B_u	0.9849
	1	146.637	A_u	0.9836
	1	146.643	A_g	0.9834
ν_{rock}	0	136.802	A_u	0.9848
	1	153.927	B_g	0.9699
	1	153.964	B_u	0.9701
$2\nu_{inversion}$	0	200.222	B_u	0.9847
	1	203.945	A_g	0.9628
	1	203.959	A_u	0.9312
$\nu_{inversion}+\nu_{stretch}$	0	209.464	A_g	0.9712
	1	218.272	B_g	0.9674
	1	218.368	B_u	0.9695

[a] ΔE is a state's energy in cm^{-1} relative to that of the lowest-energy J=1 state in the ν_3 manifold. The latter is at an energy of 3750.273 cm^{-1} relative to the J=1 ground state of the dimer.

lying intermolecular rovibrational states in each of the intramolecular vibrational manifolds considered. The J=1, K=0 intermolecular states of the HH and DH dimers in both ground and excited intramolecular vibrational states, are very close in energy, to within 0.5 cm^{-1}, to their J=0 counterparts. The K=1 intermolecular states appear as closely spaced doublets, separated by a fraction of a wavenumber. In all cases, the energy of the K=1 state is 5−19 cm^{-1} higher than that of the corresponding J=1, K=0 state. Their energy differences $E_{J=1,|K|=1}-E_{J=1,K=0}$ vary strongly, relative to that for the intermolecular ground state, for the lowest-energy intermolecular modes $\nu_{inversion}$, $\nu_{stretch}$, ν_{rock}, and the overtone $2\nu_{inversion}$. These variations are explained qualitatively by considering how the excitation of each mode affects the vibrationally averaged positions of the H atoms of water, which in turn change the magnitude of the A rotational constant of the dimer and thus the difference $E_{J=1,|K|=1}-E_{J=1,K=0}$. In a few

TABLE XI Average $E_{J=1,|K|=1}-E_{J=1,K=0}$ energy differences for selected low-energy intermolecular states in the manifolds of the intramolecular vibrational states of the HH dimer. They are based on the results shown in Tables I−VI.

	S_0[a]	ν_2	ν_1	ν_3	ν_{HCl}
Ground state	13.738	13.849	13.442	13.586	13.279
$\nu_{inversion}$	9.280	8.843	9.338	9.352	10.388
$\nu_{stretch}$	13.771	13.883	13.485	13.615	13.883
ν_{rock}	18.482	18.940	17.870	18.382	16.782
$2\nu_{inversion}$	5.155	4.483	5.486	5.474	4.483

[a] S_0 refers to the ground state.

TABLE XII Average $E_{J=1,|K|=1}-E_{J=1,K=0}$ energy differences for selected low-energy intermolecular states in the manifolds of the intramolecular vibrational states of the DH dimer. They are based on the results shown in Tables II−X.

	S_0[a]	ν_2	ν_1	ν_3	ν_{DCl}
Ground state	13.733	13.814	13.309	13.581	14.831
$\nu_{inversion}$	8.860	8.277	9.008	9.038	10.020
$\nu_{stretch}$	13.876	13.863	13.821	13.614	13.370
ν_{rock}	17.366	17.988	16.684	17.144	16.686
$2\nu_{inversion}$	3.148	2.129	3.688	3.730	4.066

[a] S_0 refers to the ground state.

DOI:10.1063/1674-0068/cjcp2110189 ©2021 Chinese Physical Society

instances, the coupling between K=1 intermolecular vibrational states belonging to two different intramolecular vibrational manifolds results in fine splitting of certain K=1 states.

Finally, we demonstrate that the HCl and DCl stretch fundamentals in the HH and DH dimers, respectively, have virtually identical fractional vibrational frequency shifts, in accord with the prediction of the simple perturbative treatment by Buckingham of the solvent-induced frequency shifts of diatomic solutes [52, 53].

The calculations in this paper, together with the earlier ones of the 9D J=0, 1 rovibrational states of H_2O/D_2O-CO [26] and HDO-CO [29], demonstrate the maturity and the versatility of our methodology for full-dimensional and fully coupled quantum calculations of the rovibrational eigenstates of noncovalently bound diatom-triatom molecular complexes, for both the ground and excited intramolecular vibrational states of the monomers.

V. ACKNOWLEDGMENTS

Zlatko Bačić and Peter M. Felker are grateful to the National Science Foundation for its partial support of this research through the Grants CHE-2054616 and CHE-2054604, respectively. Peter M. Felker is grateful to Prof. Daniel Neuhauser for his support.

[1] A. K. Samanta, Y. Wang, J. S. Mancini, J. M. Bowman, and H. Reisler, Chem. Rev. **116**, 4913 (2016).
[2] R. P. de Tudela and D. Marx, Phys. Rev. Lett. **119**, 223001 (2017).
[3] A. C. Legon and L. C. Willoughby, Chem. Phys. Lett. **95**, 449 (1983).
[4] Z. Kisiel, B. A. Pietrewicz, P. W. Fowler, A. C. Legon, and E. Steiner, J. Phys. Chem. A **104**, 6970 (2000).
[5] M. Weimann, M. Farnik, and M. A. Suhm, Phys. Chem. Chem. Phys. **4**, 3933 (2002).
[6] M. Fárník, M. Weimann, and M. A. Suhm, J. Chem. Phys. **118**, 10120 (2003).
[7] A. J. Honeycutt, R. J. Strickland, F. Hellberg, and R. J. Saykally, J. Chem. Phys. **118**, 1221 (2003).
[8] M. Ortlieb, Ö. Birer, M. Letzner, G. D. Schwaab, and M. Havenith, J. Phys. Chem. A **111**, 12192 (2007).
[9] D. Skvortsov, S. J. Lee, M. Y. Choi, and A. F. Vilesov, J. Phys. Chem. A **113**, 7360 (2009).
[10] S. D. Flynn, D. Skvortsov, A. M. Morrison, T. Liang, M. Y. Choi, G. E. Douberly, and A. F. Vilesov, J. Phys. Chem. Lett. **1**, 2233 (2010).
[11] A. M. Morrison, S. D. Flynn, T. Liang, and G. E. Douberly, J. Phys. Chem. A **114**, 8090 (2010).
[12] M. Letzner, S. Gruen, D. Habig, K. Hanke, T. Endres, P. Nieto, G. Schwaab, L. Walewski, M. Wollenhaupt, H. Forbert, D. Marx, and M. Havenith, J. Chem. Phys. **139**, 154304 (2013).
[13] B. E. Casterline, A. K. Mollner, L. C. Ch'ng, and H. Reisler, J. Phys. Chem. A **114**, 9774 (2010).
[14] A. K. Samanta, L. C. Ch'ng, and H. Reisler, Chem. Phys. Lett. **575**, 1 (2013).
[15] M. J. Packer and D. C. Clary, J. Phys. Chem. **99**, 14323 (1995).
[16] S. Re, Y. Osamura, Y. Suzuki, and H. F. Schaefer III, J. Chem. Phys. **109**, 973 (1998).
[17] G. M. Chaban, R. B. Gerber, and K. C. Janda, J. Phys. Chem. A **105**, 8323 (2001).
[18] M. E. Alikhani and B. Silvi, Phys. Chem. Chem. Phys. **5**, 2494 (2003).
[19] M. Masia, H. Forbert, and D. Marx, J. Phys. Chem. A **111**, 12181 (2007).
[20] Y. Liu, J. Li, P. M. Felker, and Z. Bačić, Phys. Chem. Chem. Phys. **23**, 7101 (2021).
[21] J. S. Mancini and J. M. Bowman, J. Chem. Phys. **138**, 121102 (2013).
[22] B. Jiang, J. Li, and H. Guo, Int. Rev. Phys. Chem. **35**, 479 (2016).
[23] B. Jiang and H. Guo, J. Chem. Phys. **139**, 054112 (2013).
[24] J. Li, B. Jiang, and H. Guo, J. Chem. Phys. **139**, 204103 (2013).
[25] P. M. Felker, Y. Liu, J. Li, and Z. Bačić, J. Phys. Chem. A **125**, 6437 (2021).
[26] P. M. Felker and Z. Bačić, J. Chem. Phys. **153**, 074107 (2020).
[27] P. M. Felker and Z. Bačić, J. Chem. Phys. **151**, 024305 (2019).
[28] D. Lauvergnat, P. M. Felker, Y. Scribano, D. M. Benoit, and Z. Bačić, J. Chem. Phys. **150**, 154303 (2019).
[29] P. M. Felker and Z. Bačić, J. Phys. Chem. A **125**, 980 (2021).
[30] Z. Bačić and J. C. Light, J. Chem. Phys. **85**, 4594 (1986).
[31] Z. Bačić and J. C. Light, J. Chem. Phys. **86**, 3065 (1987).
[32] Z. Bačić, R. M. Whitnell, D. Brown, and J. C. Light, Comput. Phys. Commun. **51**, 35 (1988).
[33] Z. Bačić and J. C. Light, Annu. Rev. Phys. Chem. **40**, 469 (1989).
[34] D. H. Zhang, Q. Wu, J. Z. H. Zhang, M. von Dirke, and Z. Bačić, J. Chem. Phys. **102**, 2315 (1995).
[35] Y. Qiu and Z. Bačić, J. Chem. Phys. **106**, 2158 (1997).
[36] S. Carter and N. C. Handy, Comput. Phys. Commun. **51**, 49 (1988).

DOI:10.1063/1674-0068/cjcp2110189 ©2021 Chinese Physical Society

[37] X. G. Wang and T. Carrington Jr., J. Chem. Phys. **119**, 101 (2003).
[38] X. G. Wang and T. Carrington Jr., J. Chem. Phys. **129**, 234102 (2009).
[39] X. G. Wang and T. Carrington, J. Chem. Phys. **148**, 074108 (2018).
[40] P. M. Felker, D. Lauvergnat, Y. Scribano, D. M. Benoit, and Z. Bačić, J. Chem. Phys. **151**, 124311 (2019).
[41] P. M. Felker and Z. Bačić, J. Chem. Phys. **152**, 014108 (2020).
[42] P. M. Felker and Z. Bačić, J. Chem. Phys. **152**, 124103 (2020).
[43] G. Brocks, A. van der Avoird, B. T. Sutcliffe, and J. Tennyson, Molec. Phys. **50**, 1025 (1983).
[44] B. R. Johnson and W. P. Reinhardt, J. Chem. Phys. **85**, 4538 (1986).
[45] Z. Bačić, D. Watt, and J. C. Light, J. Chem. Phys. **89**, 947 (1988).
[46] B. T. Sutcliffe and J. Tennyson, Int. J. Quantum Chem. **39**, 183 (1991).
[47] X. G. Wang and T. Carrington, J. Chem. Phys. **146**, 104105 (2017).
[48] X. G. Wang and T. Carrington Jr., J. Chem. Phys. **134**, 044313 (2011).
[49] J. Echave and D. C. Clary, Chem. Phys. Lett. **190**, 225 (1992).
[50] H. Wei and T. Carrington Jr., J. Chem. Phys. **97**, 3029 (1992).
[51] A. R. Hoy and P. R. Bunker, J. Mol. Spectrosc. **74**, 1 (1979).
[52] A. D. Buckingham, Proc. Roy. Soc. A **248**, 169 (1958).
[53] A. D. Buckingham, Trans. Faraday Soc. **56**, 753 (1960).

DOI:10.1063/1674-0068/cjcp2110189 ©2021 Chinese Physical Society